INVESTIGATION OF PHOTOVOLTAIC PROPERTIES of p-InSe/n-CdS HETEROJUNCTION SOLAR CELLS

K. YILMAZ*
Pamukkale University, Science and Arts Faculty, Physics Dept., Kınıklı-Denizli Turkey 20020

In this work, n-CdS/p-InSe heterojunction structures were fabricated by successive thermal evaporation of CdS and InSe powders. The photovoltaic properties of SnO_2/n-CdS/p-InSe/Metal sandwich structures were investigated through I-V, C-V and spectral response measurements. Various metal point contacts such as Ag, Au, In, Al and C were deposited onto amorphous InSe films by thermal evaporation technique. The best photovoltaic behaviors were observed with Au and C contacts. Other metals showed ohmic current–voltage characteristics and poor photovoltaic responses. Solar cell parameters of the rectifying structures, SnO_2/n-CdS/p-InSe/Au and SnO_2/n-CdS/p-InSe/C under AM1 conditions were investigated. The open-circuit voltages and short-circuit currents were found to be around 400 mV and 10 $\mu A/cm^2$, respectively. Device efficiencies were limited due to the high resistivity of InSe absorber layer.

(Received March 27, 2014; Accepted April 30, 2014)

Keywords: Photovoltaics, Thin film, Heterojunction, InSe, CdS.

1. Introduction

The study of layered compounds in photovoltaics has experienced great developments in the last decade. In recent years, InSe layered semiconductors of the III-VI family have been a subject of interest both in thin film and single-crystalline form because of certain properties that make it attractive for device applications. Each layer is formed in packets of two In and two Se sublayers and the interlayer (Se-Se) bonding is of the Van der Waals type, while inside the layers the bonding is largely covalent. Due to this bonding scheme, no dangling bonds exist at the surface which is an ideal condition for fabricating metal-semiconductor or p-n heterojunctions. Thus, the interfaces between such layered materials are unstrained even for the relatively high lattice mismatches [1]. The possibility of obtaining p- and n-type conduction with doping makes InSe is a promising material for p-n heterojunction device structures with a low density of interface states [2]. Moreover, with a room temperature band gap about 1.3 eV which is close to the solar optimum, InSe is an appropriate material for photovoltaic conversion [3]. The structural and electrical properties of InSe thin films, which strongly affect the device performance, depend on the deposition techniques and conditions [4]. The understanding of the electrical parameters of the material, considerably influenced by the presence of energy levels in the forbidden gap which was studied in our previous work using (SCLC) Space-charge-limited current measurements technique [5].

Despite the fact that InSe films and associated devices has been studied by a large number of workers, most of the work done considered the single crystal forms or n-type polycrystalline films and a very little information is known about the photovoltaic effect in amorphous thin film semiconductors. In this work; device properties of TO/CdS/a-InSe/Metal heterojunction structures have been investigated.

*Corresponding author: kyilmaz@pau.edu.tr

2. Experimental

In order to achieve n-CdS/p-InSe heterojunction structure, polycrystalline CdS thin films were evaporated by thermal evaporation onto SnO_2 (TO) coated glass substrates. Following to this process amorphous InSe thin films were evaporated onto CdS films and finally, various electrodes such as Au, Ag, In and Al were achieved onto the p-InSe thin films as top point contacts whose area is around $8x10^{-3}$ cm^2. For the deposition of InSe films , 99.99 % pure In_2Se_3 single crystal powder which is kept at around 800 ^oC under 10^{-5} Torr were used. Later, (liquid colloidal graphite) C point contacts were pasted on to the films as cold contacts. Prior to device characterization structural, electrical and optical properties of the InSe and CdS thin films were determined. Structural analyses of the films were carried out by using JSM-6400 scanning electron microscope (SEM) equipped with energy dispersive X-ray facility (EDXA) and Rigaku Miniflex X-ray diffractometer (XRD). Electrical properties of both films and the devices were carried out using Keithley 220 constant current source and Keithley 619 electrometer. Temperature dependent current-voltage characteristics were done by Janis liquid nitrogen VPF series crysostat. The Hall effect measurements of the films were carried out by the same system except a constant magnetic field of 0.97 T applied parallel to the c-axis (perpendicular to the film surface) using Walker Magnion model FCC-4D magnet. Optical properties were studied by means of transmission-absorption and spectral response measurements. The transmission-absorption measurements were done by a double beam Perkin-Elmer UV/VIS lambda 2S spectrometer. Spectral response analyses were performed by using an Oriel MS 257 monochromator together with HP 4140 picoammeter/dc voltage source [6].

3. Results and Discussion

3.1. InSe and CdS film properties.

The structural properties of the deposited InSe and CdS thin films were examined through SEM and EDXA analysis. EDXA analysis have shown that as-grown InSe films were composed of about 49% In and 51% Se and no other impurity atoms found in the structure. XRD and electrical measurements have indicated that undoped InSe thin films deposited on cold substrates were amorphous with p-type conductivity lying in the range of 10^{-4}-10^{-5} $(\Omega.cm)^{-1}$ at room temperature [7]. The temperature dependent I-V and Hall effect measurements have shown that conductivity and carrier concentration increases with increasing absolute temperature while mobility is almost temperature independent in the studied temperature range of 100-430 K which reveals that the dominant scattering mechanism is neutral impurity scattering. Carrier concentration and mobility values of InSe films at room temperature were determined to be in the range of 10^{12}-10^{13} cm^{-3} and 2.7-82 cm^2/V.s, respectively. The conduction mechanisms of the InSe films were also investigated in temperature region of 100-430 K. It was found that thermal excitation is dominant above 200 K in which region conductivity increases sharply with temperature whereas below 200 K, temperature dependence is weak and conduction dominated by variable-range hopping (VRH) [6].

Structural properties of CdS thin films deposited by thermal evaporation technique were also analyzed for the purpose of p-n heterojunction device investigations. XRD pattern of all deposited CdS films revealed that the films were polycrystalline with a preferred direction of crystallinity in (*002*) plane that is consistent with previous works [8]. The observed reflection peak can be attributed to the typical (*00l*) lines of the hexagonal structure of CdS. The temperature dependent electrical conductivity and Hall Effect measurements in the range of 100-430 K were also studied for CdS thin films. All deposited CdS films exhibited n-type conductivity and room temperature conductivity values were found to be around 1 $(\Omega.cm)^{-1}$ [9]. The variation of conductivity of CdS films were found to be increasing exponentially with increasing temperature. Above 200 K, thermionic emission was determined to be the dominant conduction mechanism while below 200 K, it was found to be VRH. Room temperature electron concentrations and Hall mobility of the CdS thin films were found to be lying in the range of 10^{16}-10^{18} cm^{-3} and 3.1-3.5

cm^2/V.s, depending on the substrate temperatures [10]. The grain boundary height was calculated to be 98 meV and 14 meV in the high and low temperature regions, respectively. The dominant scattering mechanism in the low temperature region was found to be neutral impurity scattering as in this region mobility variation was almost independent of absolute temperature. In the high temperature region, the variation fits to ionized impurity scattering that may be attributed to the increase in the ionization of impurities with increasing temperature thus scattering of carriers by impurities occurs. Through the transmission-absorption measurements, optical band gaps of CdS and amorphous InSe films were determined to be around 2.4 and 1.7 eV, respectively [11,12].

3.2. TO/CdS/a-InSe/Metal heterojunction devices.

The photovoltaic properties of n-CdS/p-InSe heterostructures with various top electrodes were investigated. The best photovoltaic behaviors observed for the Au and C contacts. In, Al and Ag top contacts showed ohmic behavior and poor photovoltaic response. The ideality factor for the heterostructure with Au contact was found to be around 2.4 and a reverse saturation current of $3x10^{-11}$ A, as seen in figure1.

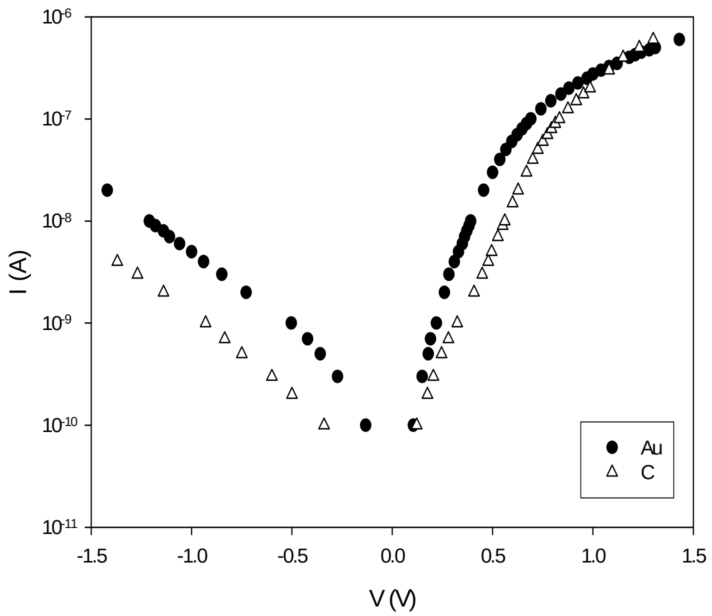

Fig. 1. Typical forward-reverse I-V characteristics of TO/n-CdS/p-InSe/(Au, C) system.

The I-V characteristics of this structure under illumination at AM1 condition (100 mW/cm^2) indicated an open-circuit voltage (V_{oc}) around 400 mV and short-circuit current (I_{sc}) of $4.9x10^{-8}$ A (~ 6 $\mu A/cm^2$), shown in figure 2. The efficiency of the solar cell was quite low with a fill factor (FF) of 0.44 which is due to the small short-circuit current that is limited by the high resistivity of the InSe absorber layer. Typical TO/CdS/a-InSe/C heterostructures had quite similar characteristics as the ones with Au top contacts, also shown in figure 1 and figure 2.

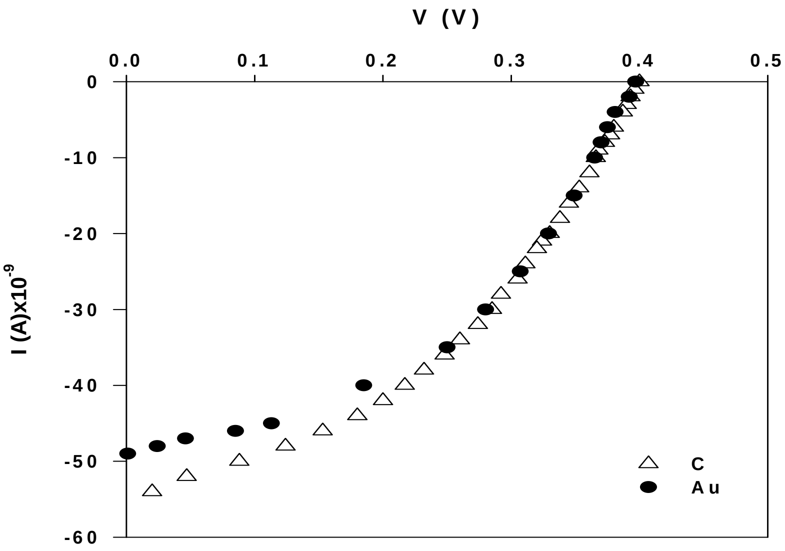

Fig. 2. Illuminated I-V characteristics of TO/n-CdS/p-InSe/(Au, C) system.

The ideality factor for the cell with C electrode was found to be 2.9 and the reverse saturation current was of the order of $2x10^{-11}$ A. The V_{oc} and I_{sc} for this structure was determined from the illuminated I-V characteristics around 400 mV and $5.4x10^{-8}$ A (~ 7 μA/cm^2), respectively. The FF for this system was found to be 0.41 that is comparable to the heterostructure with Au top electrode. C-V and C-f measurements have been carried out in the frequency range of 1-2000 kHz and it was found that both structures have similar behaviors. The capacitance in the reverse bias region varied slightly whereas in the forward region increases with increasing voltage, as shown in figure 3.

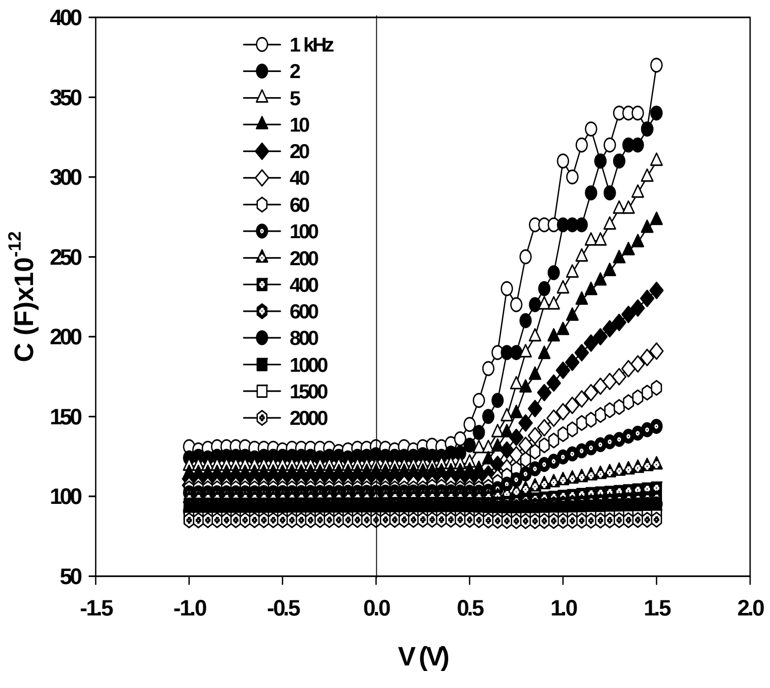

Fig. 3. C-V variation of a typical TO/n-CdS/p-InSe/Au solar cell at various frequencies.

This is attributed to the high resistivity of InSe layer and the change of capacitance in the forward bias region is due to the change of the depletion region in CdS side. C-V dependence is weak at high frequencies. The built-in potential for TO/n-CdS/p-InSe/Au system in the frequency range of 1-20 kHz was found to be in between 0.85-1.10 V from the C^{-2}-V plot, as seen in figure 4.

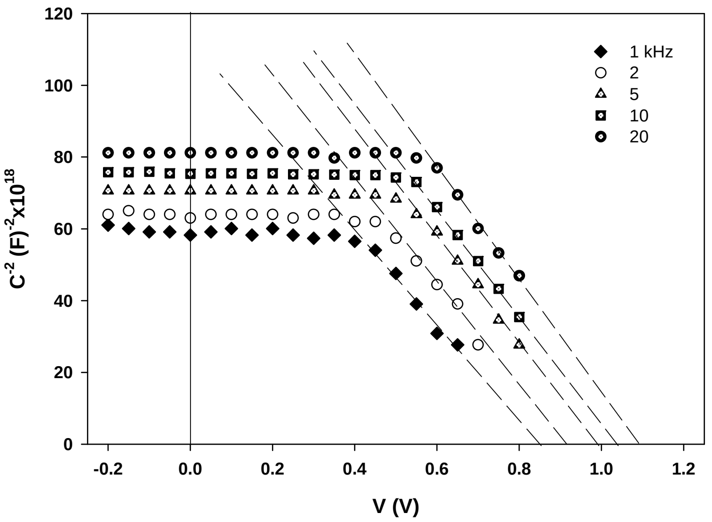

Fig. 4. C^{-2}-V variation for TO/n-CdS/p-InSe/Au solar cell in frequency range of 1-20 kHz.

This variation of the built-in potential with frequency was explained through the effect of interface states at the junction. The values of the built-in potentials were higher than the theoretically calculated value of 0.7 V which indicates the presence of a relatively thick interfacial layer. Besides, as indicated in figure 5, frequency dependence of the capacitance is stronger for the low frequencies than for higher frequencies that is an indication of presence of interface states at the junction because at high frequencies ac signal could not be followed by the interface states.

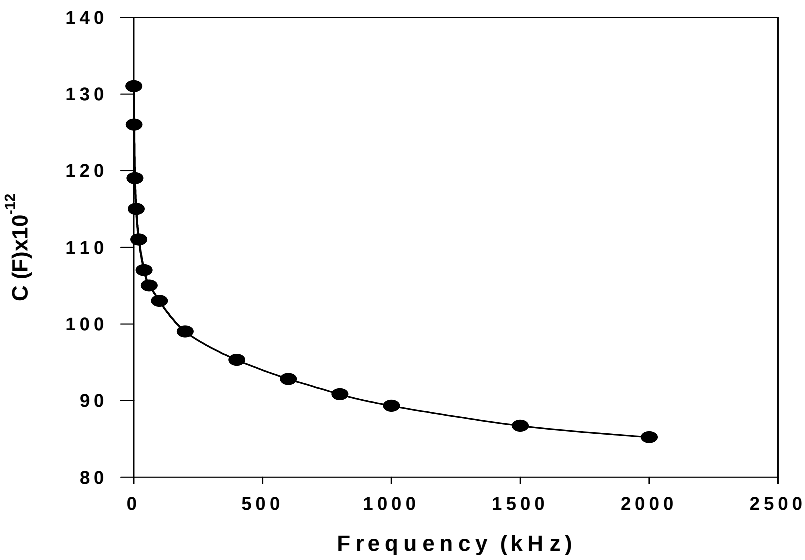

Fig. 5. Junction capacitance-frequency variation for a typical TO/n-CdS/p-InSe/Au solar cell in the range of 1 kHz- 2 MHz at zero bias.

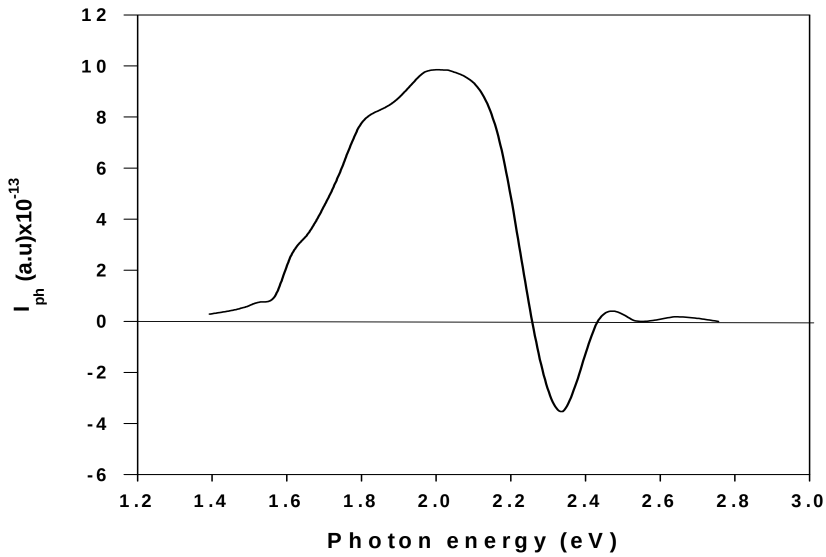

Fig. 6. The spectral distribution of a TO/n-CdS/p-InSe/Au system at zero bias.

The photocurrent measurement of a typical cell was carried out in the wavelength range of 450-900 nm. In figure 6, the spectral response curve indicates two broaden peaks one at around 1.9 eV and other one at 2.4 eV which are attributed to band-to-band transitions. The negative peak which comes from the CdS layer can be explained by the recombination of majority carriers at the interface with minority carriers. Thus, at wavelengths of sufficient energy to excite carriers in CdS but not in InSe, photoexcited carriers in CdS produces a photocurrent which results in a negative photoconductivity. The Fowler plot, in figure 7, reveals the barrier height at around 1.1 eV which is comparable to the value obtained from C-V analysis.

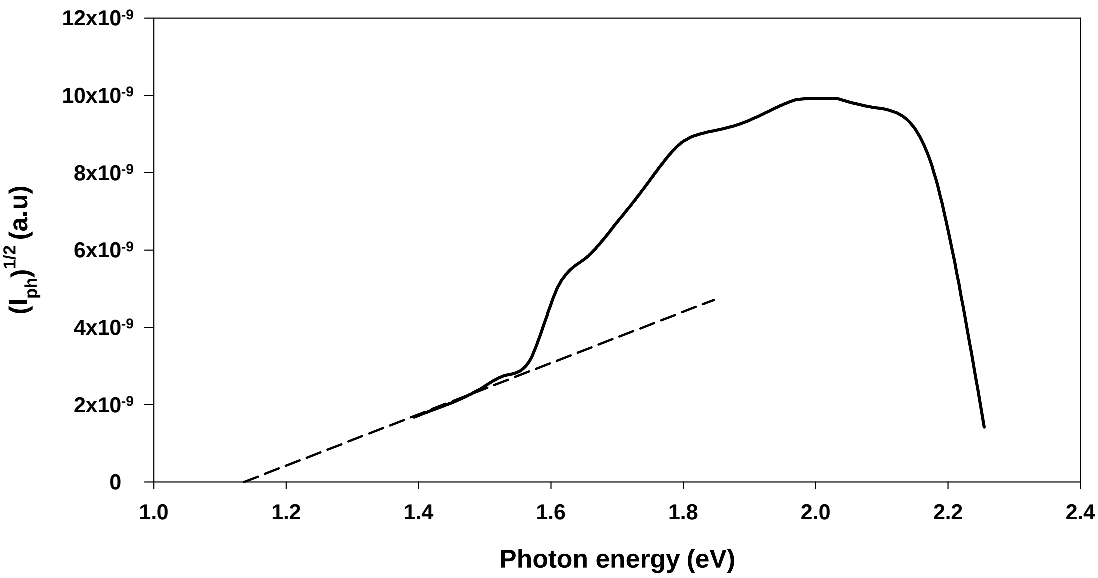

Fig. 7. The Fowler plot of a typical TO/n-CdS/p-InSe/Au cell at the threshold energy of the spectrum.

4. Conclusion

In this work, amorphous InSe and CdS thin films were successively deposited by thermal evaporation and structural, electrical and optical properties of the films were studied. Polycrstalline n-CdS and amorphous p-InSe thin film heterojunction solar cells were fabricated and photovoltaic properties were investigated with various top electrodes. Despite the fact that a reasonable barrier around 1 eV was formed between layers, it was observed that the efficiency is quite low due to the high resistivity of InSe layer which also results in high series resistance effect under illumination in the devices. C-V and C-f measurements of the cells have shown that a relatively thick interfacial layer exists limiting the short-circuit current via recombinations at interface states near or at the junction.

Acknowledgement

The author would like to thank Dr. M. Parlak and Dr. Ç. Erçelebi for their valuable suggestions throughout this work.

References

[1] A. Segura, J. P. Guesdon, J. M. Besson and A. Chevy, J. Appl. Phys., **54**(2), 876 (1983).
[2] J. Martinez-Pastor, A. Segura, J. L. Valdes and A. Chevy, J. Appl. Phys., **62,** 539 (1987).
[3] M. Di Guilio , G. Micocci, A. Rizzo and A. Tepore, J. App. Phys., **54,** 273 (1983).
[4] M. Parlak and Ç. Erçelebi, Thin Solid Films, **322,** 334 (1998).
[5] K. Yılmaz, M. Parlak, Ç. Erçelebi, J. of Mater. Sci.: Materials in Electronics, **15**, 225 (2004).
[6] K.Yılmaz, M. Parlak, Ç. Erçelebi, Semicond. Sci. Technol., 22, 1268 (2007).
[7] A. F. Qasrawi, M. Parlak, Ç. Erçelebi, İ. Günal, J. of Mater. Sci.: Materials in Electronics, **12,** 473 (2001).
[8] M. Parlak, Effects of Growth on the Properties of CdS Thin Films, M.Sc. Thesis, METU (1992).
[9] N. G. Dhere and N. R. Parikh, Thin Solid Films, **60,** 257 (1979).
[10] C. Wu and R. H. Bube, J. Appl. Phys., **45,** 648 (1974).
[11] K. Senthil, D. Mangalaraj, S. K. Narayandass, Applied Surface Science, **169,** 476 (2001).
[12] A. Chaiken, K. Nauka, G. A. Gibson, H. Lee, C. C. Yang, J. Wu, J. W. Ager, K. M. Yu W. Walukiewicz, J. Appl. Phys., **94**(4)**,** 2390 (2003).